DENTAL MATERIALS 35 (2019) 751–762

Available online at www.sciencedirect.com

ScienceDirect

journal homepage: www.intl.elsevierhealth.com/journals/dema

Long-term *in vitro* degradation behavior and biocompatibility of polycaprolactone/ cobalt-substituted hydroxyapatite composite for bone tissue engineering

Wei-Chun Lin[a], *Chenmin Yao*[b], *Ting-Yun Huang*[a], *Shih-Jung Cheng*[d], *Cheng-Ming Tang*[a,c,*]

[a] *Graduate Institute of Oral Science, Chung Shan Medical University, Taichung 40201, Taiwan*
[b] *The State Key Laboratory Breeding Base of Basic Science of Stomatology (Hubei-MOST) & Key Laboratory for Oral Biomedicine Ministry of Education, School & Hospital of Stomatology, Wuhan University, Wuhan, China*
[c] *Chung Shan Medical University Hospital, Taichung 40201, Taiwan*
[d] *Department of Dentistry, Chung Shan Medical University, Taiwan*

ARTICLE INFO

Article history:
Received 23 December 2018
Accepted 13 February 2019

Keywords:
Polycaprolactone
Cobalt-substituted hydroxyapatite
Biodegradation
Bone induction
Antibacterial
Anti-inflammatory

ABSTRACT

Objective. Currently, infections due to foreign-body reactions caused by bacteria or implant materials at the wound site are one of the major reasons for the failure of guided tissue regeneration (GTR) and guided bone regeneration (GBR) in clinical applications. The purpose of this study was to develop regeneration membranes with localized cobalt ion release to reduce infection and inflammation by polycaprolactone (PCL)/cobalt-substituted hydroxyapatite (CoHA).

Methods. The PCL composite membrane containing 20 wt% CoHA powders was prepared by solvent casting. The surface morphology, crystal structure, chemical composition and thermal properties of PCL composite membranes were characterized. The biocompatibility, osteogenic differentiation and antibacterial properties of composite membrane were also investigated. Then, in biodegradability was assessed by immersing phosphate buffer solution (PBS) for 6 months.

Results. Physicochemical analyses revealed that CoHA is evenly mixed in the membranes and assistance reduce the crystallinity of PCL for getting more degradation amounts than PCL membrane. Osteoblast cells culture on the membrane showed that the CoHA significantly increases cell proliferation and found the calcium deposition production increased over 90% compared with PCL after 7 days of culture. A good antibacterial effect was achieved by the addition of CoHA powder. The results were confirmed by 2.4 times reduction of proliferation of *Escherichia coli* (*E. coli*) seeded on the composite membrane after 24 h. Immersing in PBS for 6 months indicated that PCL–CoHA composite membrane has improved biodegradation and can continuously remove free radicals to reduce the inflammatory response.

* *Corresponding author at*: Graduate Institute of Oral Science, Chung Shan Medical University, No. 110, Sec. 1, Jianguo N. Rd., Taichung, 402, Taiwan.
E-mail addresses: tukust94114wenny@gmail.com (W.-C. Lin), yao_chenmin@whu.edu.cn (C. Yao), miumiu_0516@hotmail.com (T.-Y. Huang), amyc1101@gmail.com (S.-J. Cheng), ranger@csmu.edu.tw (C.-M. Tang).
https://doi.org/10.1016/j.dental.2019.02.023

Significance. The PCL–CoHA composite membrane with suitable releasing of cobalt ion can be considered as a potential choice for bone tissue regeneration.

1. Introduction

In clinical dentistry, it is common to encounter patients with defects in hard bone tissues, such as defects in alveolar bone caused by trauma or tooth extraction. Clinical practices have introduced the concepts of guided tissue regeneration (GTR) and guided bone regeneration (GBR) to stomatological treatment, which is used to inhibit the growth of fibroblasts towards the bone defect site and facilitate bone regeneration by supporting the adhesion and proliferation of bone cells [1]. GTR or GBR membranes should have good biocompatibility and suitable degradation characteristics. Therefore, biodegradable polymer membranes that do not require secondary surgical removal or impose an additional burden on the patients themselves are majorly used for bone regeneration applications [2,3]. The degradation rate should also match the rate of the formation of new tissues to achieve the desirable goal of restoration [4]. Thus, using biodegradable membranes is mainstream in GTR (or GBR) treatment [5]. Currently, polycaprolactone (PCL) is an important biodegradable polymer material with a hydrophobic property, which can contribute to cell adhesion, proliferation, and interaction with biological fluids [6]. High-molecular weight PCL undergoes hydrolysis to form low-molecular weight PCL, which is engulfed by macrophages and further decomposed. PCL is widely used in drug carrier [7], cosmetic surgery [8], tissue engineering and body implant materials [9].

In addition, hydroxyapatite (HA) can be added to increase the osteoinductivity of the membrane and enhance its biological activity [10], for inducing bone tissue growth at the bone defect site [11,12]. However, infections due to foreign-body reactions caused by bacteria or implant materials at the wound site are one of the major reasons for the failure of GTR and GBR in clinical applications [13]. It is expected that the addition of HA can reduce inflammatory responses and have an anti-bacterial function, apart from enhancing the biological activity of PCL. Therefore, there are numerous literatures reporting the modification of hydroxyapatite [14,15]. The calcium ions in the structure can be displaced by divalent metal ions to change the original properties of the hydroxyapatite [16]. For example, silver dropped hydroxyapatite has an anti-bacterial effect to reduce the risk of postoperative infections [17], while strontium hydroxyapatite has been reported to help improve the healing of bone tissue in a sheep model of osteoporosis [18]. Among others, cobalt is a necessary trace element for the human body. Cobalt mainly enters the human body via the digestive and the respiratory tract, and is mostly stored in the liver, followed by the kidney and bones. The average human daily intake of cobalt from food and drinks is around 300 μg [19]. Besides, cobalt ion is an inhibitor of prolyl hydroxylase enzymes and is often used as a hypoxia-mimicking agent, which increases the protein expression of hypoxia-inducible factor (HIF-1α) effectively in a short period of time. This in turn induces the secretion of vascular endothelial growth factor (VEGF) from cells; better growth performance can be achieved by the production of VEGF [20]. Other literatures suggest that cobalt ions can increase the regeneration of blood vessels and endothelial cells in tissues [21], which is an important part of bone formation, and has a good anti-bacterial effect [22].

According to the above, this study involves the preparation of a PCL composite membrane that contains cobalt-substituted hydroxyapatite. The main objectives are: (1) to analyze the effect of cobalt-substituted hydroxyapatite on the properties of PCL and on improving the biocompatibility, anti-bacterial ability, and anti-inflammatory response of the membrane, and (2) to perform *in vitro* biodegradation tests by immersing the membrane in a phosphate buffer solution for a long time-period to investigate the degree of membrane degradation at different times and the release behaviors of cobalt ions. We hypothesized that the addition of CoHA is significantly effective for the antibacterial and anti-inflammatory properties of the membranes. This study is expected to provide useful information for the development of anti-inflammatory and anti-infective regeneration membranes.

2. Materials and methods

2.1. Preparation of Co-HA powder

The CoHA was prepared by electrochemical deposition method. The electrolyte was prepared by dissolving of 25 mM ammonium dihydrogen phosphate (Showa chemical industry, Tokyo, Japan) and 42 mM calcium nitrate (Shimada chemical works, Tokyo, Japan) and 7 mM cobalt chloride (Shimada chemical works, Tokyo, Japan) in distilled water. The Ti and 304 stainless steel were used as a cathode and an anode, respectively. The electrodeposition of the CoHA was controlled at 5 V, 55 ° for 20 min [23]. After the reaction was completed, rinsed with deionized water and dried, the powder was removed from the surface and collected.

2.2. Preparation of PCL/CoHA membrane

The polycaprolactone (PCL) (Sigma-Aldrich, Missouri, USA) (molecular weight: 80 kDa) was dissolved in 1,4-dioxane (Avantor, New Jersey, USA) at 15 wt% and stirred uniformly for 24 h at room temperature as a PCL solution. The composite polymer solution was formulated with hydroxyapatite (HA) (Acros Organics, Belgium) or CoHA in solution in an amount of 20 wt % based on the weight of the PCL. They called the PCL–HA and PCL–CoHA solution. The three solutions were each poured into a polytetrafluorethylene disc mold (90 mm in diameter), and placed in a fume hood until the solvent evaporated.

2.3. Characterization

The microstructures of the membranes surface were observed by field emission scanning electron microscope (FESEM) (JSM-6700F, JEOL, Tokyo, Japan) and the surface elements composition of the membrane were detected by energy dispersive spectrometer (EDS). The phase composition of the membranes was determined by X-ray diffractometer (XRD) (Miniflex II, Rigaku, Japan). The XRD spectra were conducted at radiation ($\lambda = 1.54$ Å) in the range of 10–60° at a scan rate of 4°/min. The specific functional group analysis of the membrane was used a Fourier transform infrared spectrometer (FTIR) (FTIR-8000, Shimadzu, Tokyo, JAPAN). FTIR spectra were obtained in the spectral range of 4000–600 cm^{-1} and a resolution of 0.5 cm^{-1}, using the ATR technique. Thermal behavior of PCL and PCL/CoHA membranes was observed with each other using a thermo gravimetric analysis (TGA) (TGA-7, Perkin Elemer, Massachusetts, USA) and differential scanning calorimetry (DSC) (2-HT, Mettler-Toledo, Greifensee, Switzerland). The measurements were carried out at cooling and heating rate of 10 °C/min from 110 °C to 800 °C.

2.4. Biocompatibility

Human osteosarcoma cell line (MG63) were used as a compatibility assessment according to the relevant specification. Moreover, using cobalt ion standard solution (AccuStandard, New Haven, USA) as a positive control. A total of 40 μL PCL, PCL–HA and PCL–CoHA solution is coated on a circular glass (15 mm in diameter) by spin coating method. Before cell seeding, all sample was sterilized with UV radiation for 1 h. The sterilized composites membranes was placed into 24-well culture plates and seeded with a cell suspension with a cell density of 5×10^4 cells/mL, followed by culturing for 24, 48 and 72 h at 37 °C in a 5% CO_2 incubator. After incubation, samples were washed using phosphate buffered saline (PBS), added MTT solution (Sigma-Aldrich, Missouri, USA) and incubated for 4 h. After removal of the medium, 0.5 mL of DMSO was added to the wells. Then 0.1 mL of supernatants was transferred into a 96-well plate for optical density (O.D.) measuring at 570 nm.

2.5. Staining for osteogenesis

The expression of calcium deposition by MG63 cells was confirmed using alizarin red staining (ARS) (Sigma-Aldrich, Missouri, USA). MG63 cells (1×10^4 cells/well) were cultured on the composites membranes for 3 and 7 days. Fixed cell with 4% paraformaldehyde for 10 min and wash with PBS for 2–3 twice. After stained with 2% ARS solution for 15 min at room temperature, the pH of ARS solution was adjusted o 4.1–4.3. Ultimate we used deionized water to clean the surface of the membranes for 2–3 times. The results of staining were observed by optical microscope. In the quantitative analysis, the ARS on the specimen after washing was dissolved in 0.2 M NaOH/methanol (1:1) to measure the optical density at 620 nm [24].

2.6. Antibacterial properties

The PCL, PCL–HA and PCL–CoHA composite membranes were investigated against *Escherichia coli* as a model Gram-negative bacteria by the colony plate count method in order to quantify the bacterial effect of our system. The *E. coli* were prepared from fresh brain heart infusion (BHI, Becton Drive, Franklin Lakes, USA) and incubated at 37 °C for 24 h. The BHI containing *E. coli* was diluted to 10^{-3} CFU/ml of its original concentration, and 1 mL of bacteria liquid was extracted and deposited onto composite membrane cut into fixed area (1 cm^2), placed into a centrifuge tube and cultivate for 18 h. After the samples were removed, 100 μL bacterial solution was extracted and applied on the BHI agar dish (Becton, Dickinson and Company, USA) before being cultured for 24 h at 37 °C [22]. Finally, the colonies were counted, and the results were expressed as percentage reduction rates bacteria number = [$\alpha \times 10^5$], where α is the number of bacterial colonies.

2.7. Free radical scavenging ability

The free radical scavenging activity of PCL composite membranes was evaluated using 2, 2-diphenyl-1-picrylhydrazyl (DPPH) (Sigma-Aldrich, Missouri, USA) [25,26]. The configuration of the free radical solution using 0.02 g of DPPH was added to 100 mL of methanol and stirred for 45 min in the dark. 1 mL distilled water (control) or 1 mL deionized water containing 0.6 cm^2 of PCL composite membrane or 1 mL composite membrane extraction solution (after immersion in the PBS) was added to 3 mL of free radical solution and allowed to react for 90 min at room temperature. The absorbance of the reaction mixture was then measured at 517 nm using UV–vis. The free radical scavenging effect was determined by the following formula [26]: scavenging ratio (%) = [1 − (absorbance of test sample/absorbance of control)] × 100%.

2.8. Statistics analysis

In this study, all data from the average of the 3 repeat samples ± standard deviation. Data were calculated using JMP11 software (North Carolina State, USA). One-way ANOVA was used to examine the differences, accompanying using the Tukey HSD multiple comparison. $p < 0.05$ is considered to have significant difference.

3. Results

3.1. Characterization of CoHA powder

The surface morphology of CoHA was observed using FESEM (Fig. 1A). The CoHA powders were spherical and densely packed together. The size of the powders is about 300–400 nm. The composition of CoHA powders is analyzed by ICP-OES (Fig. 1B). The Ca + Co/P ratio was calculated to be 1.62, similar to the Ca/P ratio of human bone (1.67). The cobalt ion contents of the CoHA powder were 13.43%. The chemical composition of CoHA by FTIR spectra is shown in (Fig. 1C). The absorption peaks at wave numbers of 564.1 cm^{-1}, and 1043 cm^{-1} represent PO_4^{3-}, while those at 3484 cm^{-1} represent representing

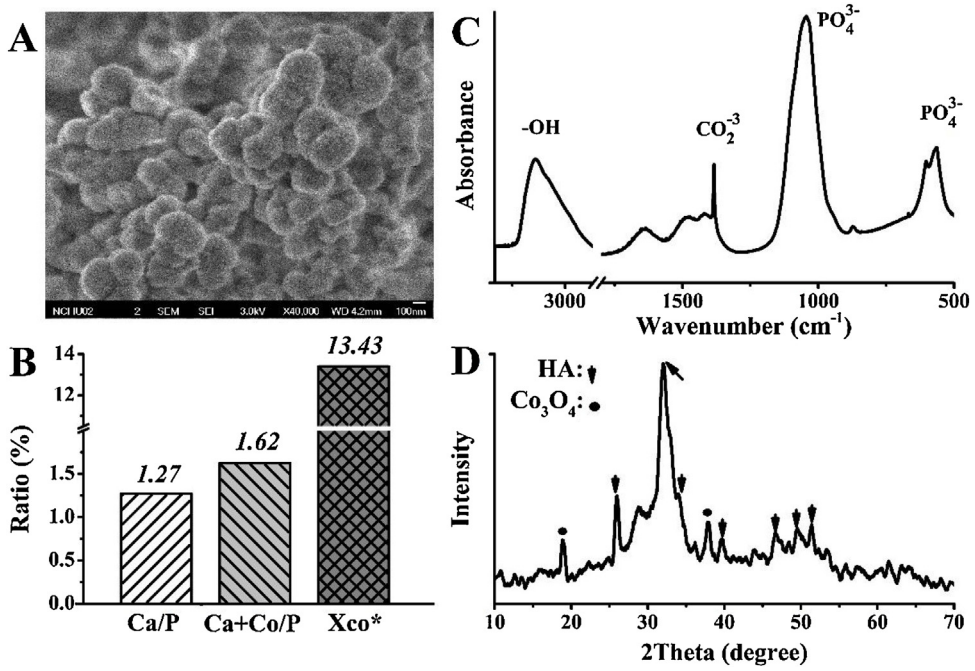

Fig. 1 – Surface topography, calcium–phosphorus ratio, chemical composition and crystal structure of the cobalt-substituted hydroxyapatite: (A) FE-SEM micrographs, (B) ICP-OES analysis, (C) FTIR spectra and (D) XRD patterns.

OH^- [27]. The peaks at 1423.3 cm^{-1} represent type B carbonate bands (CO_3^{2-}) [28]. In the previous study, CO_3^{2-} can promote the degradation of HA, provides calcium and phosphorus ions to be adsorbed during bone remodeling and assist bone growth [29]. The X-ray diffraction analysis results of the powder crystal structure are shown in Fig. 1D. It was found that there were hydroxyapatite diffraction peaks (JCPDS.No-09-0432) at 26.01°, 32.04°, 39.68°, 46.81°, and 49.74° [28], and cobalt oxide diffraction peaks (JCPDS. No-42-1467) at 18.8° [22]. Based on the above results, the existence of the CoHA structure was confirmed.

3.2. *Characterization of PCL composite*

The SEM image shows that the surface of PCL and PCL composite membranes is very flat (Fig. 2). The presence of HA or CoHA powders was observed on the membranes of PCL–HA and PCL–CoHA. The surface element compositions of PCL composite membranes were analyzed by EDS (Table 1). The presence of calcium and phosphorus elements was observed on the surfaces of PCL–HA and PCL–CoHA. Especially in PCL–CoHA, a small amount of cobalt was also found. The results of XRD patterns of PCL, PCL–HA and PCL–CoHA are shown in Fig. 3A. The two diffraction peaks located at 21.2° (110) and 23.5° (200) are assigned to crystalline of PCL [30–33]. The diffraction curve for HA is characterized two peaks located at26° (002) and 32° (211) [28,34]. According to the ATR-FTIR spectra of the PCL (Fig. 3B), the characteristic peaks of PCL appear at approximately 2949 cm^{-1} (CH_2 stretch), 2863 cm^{-1} (CH_2 stretch), 1289 cm^{-1} (C—O and C—C stretching), 1241 cm^{-1} (asymmetric —C—O— stretching) and 1171 cm^{-1} (asymmetric —C—O— stretching) [30,35]. The characteristic peaks of HA appear at approximately 1026 cm^{-1} (PO_4^{3-} stretch) [36,37]. These stretching also simultaneously appear on ATR-FTIR spectra which represent PCL–HA and PCL–CoHA composite membranes. Thermal stability of the PCL and PCL–CoHA composites membrane was assessed by the TGA and DSC curves. The TGA curves of the composite membranes are shown in Fig. 3C. The initial weight loss at 100–180 °C is associated with evaporation of water. In the PCL and PCL–CoHA composite membrane, the main weight loss happens in the temperature range 250–450 °C. At the finish of 600 °C while it was observed 82% of weight loss for the PCL–HA and PCL–CoHA composite membrane (Table 1). The content of HA and CoHA powders in the composite membrane is shown to be similar to the initial addition of 20%. The DSC thermograms are presented in Fig. 3D. The main data are summarized in Table 1. The endothermic melting enthalpies (ΔHm) of a standard PCL crystal is 139 J/g [33], and the endothermic melting enthalpies of PCL in PCL–HA and PCL–CoHA are 48.5 J/g and 52.0 J/g, respectively (Table 1). From these data, the degrees of crystallinity of PCL in PCL–HA and PCL–CoHA are calculated to be 34.8% and 37.3%, respectively (Table 1). The crystallinity of PCL decreases with the incorporation of HA and CoHA.

3.3. *Biocompatibility, differentiation and staining of osteoblast*

Previous studies have shown that the cobalt ion concentration has an impact on cell growth [38]. Therefore, we used different concentrations of the cobalt ions standard solution to evaluate cytotoxicity. The results showed that the concentration of cobalt ion below 15 ppm was not significantly toxic to the cells. However, cell growth was adversely affected when the concentration of cobalt ions in the medium reached

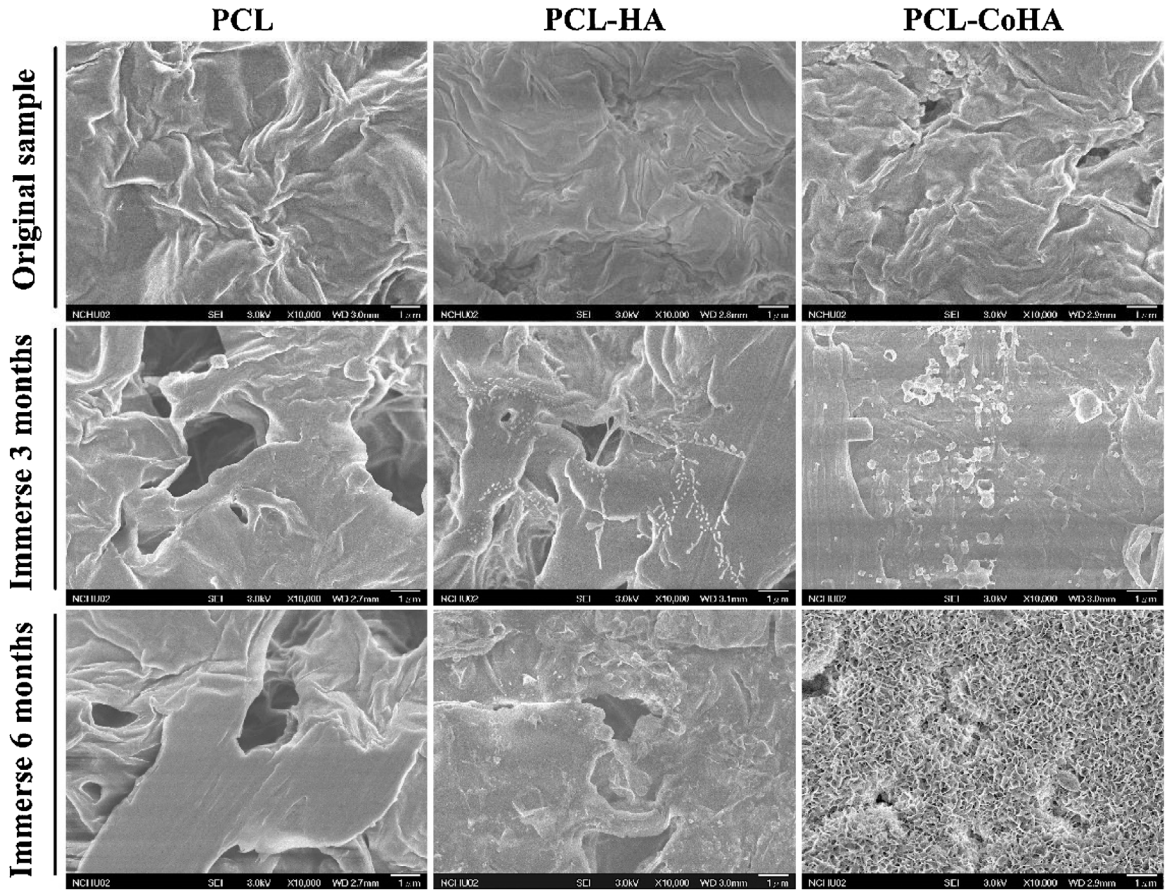

Fig. 2 – FE-SEM micrographs of PCL, PCL–HA and PCL–CoHA composites membranes and after degradation for 3 and 6 months in PBS.

Table 1 – Surface element analysis of PCL, PCL–HA and PCL–CoHA composites membranes by EDX.

Original membranes				Immerse in PBS					
				3 month			6 month		
Atomic %	Ca	P	Co	Ca	P	Co	Ca	P	Co
PCL	–	–	–	–	–	–	–	–	–
PCL–HA	0.83	0.96	–	0.77	0.83	–	1.58	1.45	–
PCL–CoHA	1.2	1.47	0.22	0.76	0.86	0.22	6.18	7.15	0.5

20 ppm (Fig. 4A). MTT assay showed that the membrane addition CoHA obviously increased the proliferation rate of Mg63 cell after 24 h compared to TCP (Fig. 4B). At 72 h the PCL–CoHA composite membrane had the highest cell numbers ($p < 0.05$). The cell numbers were up-regulated (11%) in the presence of PCL–CoHA composite membrane compared with the TCP. The osteogenic activity of Mg63 cells was then evaluation by determination calcium deposition production. The alizarin red staining of membranes that had been cultured for 7 days revealed enhanced calcium deposition within the PCL–HA and PCL–CoHA composite membrane compared with the pure PCL (Fig. 4C). The quantitative results of calcium deposition after 7 days of cell culture are shown in Fig. 5D. The calcium deposition production was up-regulated (2 multiples) in the presence of PCL–CoHA composite membrane compared with the TCP. Therefore, the results show that the addition of CoHA powder contributes to calcium deposition ($p < 0.05$).

3.4. *Antibacterial activity*

The *E. coli* cultured with 1 cm^2/mL of PCL, PCL–HA and PCL–CoHA composite membranes for 18 h, then alive bacteria were observed by culturing in agar plates for 24 h (Fig. 5A–D). Significant reduction in bacterial colonies is observed in the agar plates of the PCL–CoHA group. The quantitative result of CFU is displayed in Fig. 5E. The highest antibacterial effect was observed of PCL–CoHA ($p < 0.05$). That PCL–CoHA group eminently reduced the bacteria viability almost by 66% compared to the control group.

3.5. *In vitro biodegradation*

The surface topography of PCL, PCL–HA and PCL–CoHA composite membranes after 3 and 6 months degradation by FE-SEM (Fig. 2). In the PCL–HA group, there are some irregular

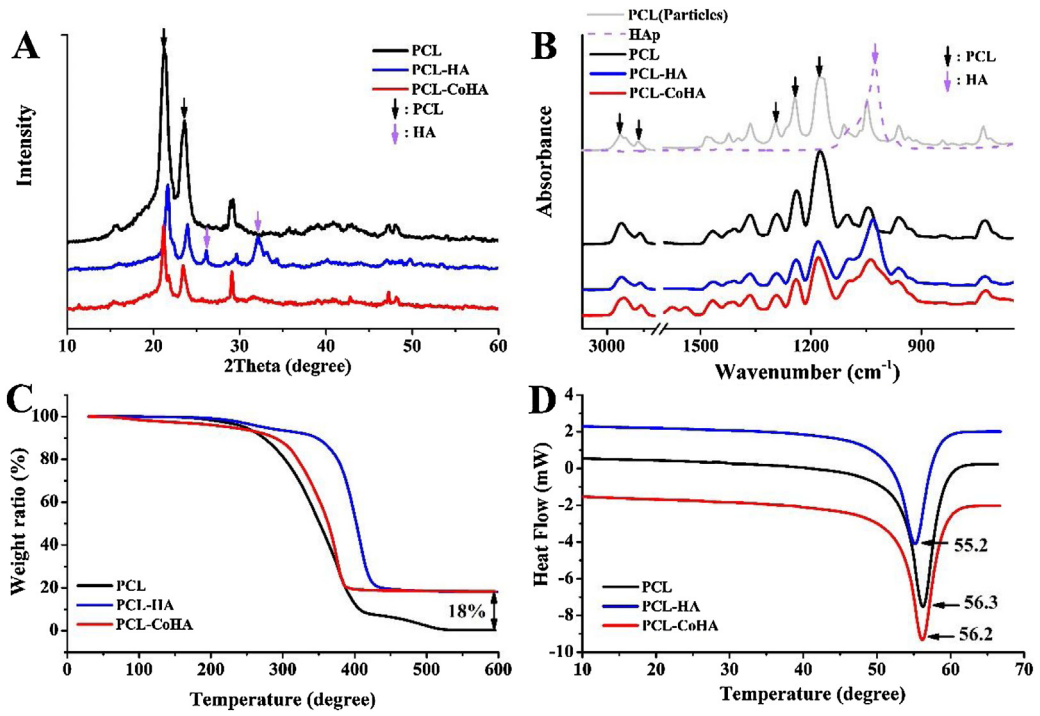

Fig. 3 – The crystal structure, chemical composition and thermal properties of PCL, PCL–HA and PCL–CoHA composites membranes: (A) XRD patterns, (B) ATR-FTIR spectra, (C) TGA curves and (D) DSC thermograms.

Table 2 – Thermal properties of PCL, PCL–HA and PCL–CoHA composites membranes by TGA and DSC.

Sample	T_{onset} (°C)	T_p (°C)	Ash (%)	T_c (°C)	T_m (°C)	ΔH_m (J/g)	Xc (%)
PCL	246.6	351.2	0.2	37.1	56.3	55.0	39.4
PCL–HA	272.3	402.3	18.1	38.2	55.2	48.5	34.8
PCL–CoHA	224.2	363.1	18.2	38.8	56.2	52.0	37.3

T_{onset}: onset temperature of pyrolysis, obtained from TGA curves at 95% weight.
T_p: peak pyrolytic temperature, obtained from TGA curves at 50% weight.
Ash content (%) = PCL–HA and PCL–CoHA deduction PCL in 600° (%), crystallization temperature (T_c), melting temperature (T_m) and enthalpy of crystallization of PCL (ΔH_m), obtained from DSC.

crystals on the surface apart from similar pores. Interestingly, the PCL–CoHA group did not observe holes on the surface after 3 months' soaking, instead more irregular crystals appeared. Simultaneously the PCL–CoHA composite membranes surface is covered by needle crystals after six months' soaking PBS. EDS analysis shows that these crystals are calcium phosphate crystals (Table 1). The pH value of PCL composite membrane soaked in PBS at different times is shown in Fig.6A. The results display that the pH value of PBS decreases with time. However, PCL–HA and PCL–CoHA have higher pH value than pure PCL due to degradation of HA. After 6 months of soaking, the weight loss of all groups is less than 10% (Fig. 6B), but PCL–HA and PCL–CoHA composite membranes showed more weight loss ($p < 0.05$). This result is consistent with the change in pH, an addition of HA and CoHA increases the weight loss of the membranes and slows down the decrease in pH value. There was no difference in the chemical composition on the surface of pure PCL and PCL–HA composite membranes after degradation at different times. However, PCL–CoHA composite membranes only observed phosphate groups on the surface after 6 months of degradation (Fig. 7A–B). The result of the crystal structure analysis is shown in Fig. 7C–E. The intensity of the diffraction peak of the PCL membranes was observed as an evaluation of the crystal structure. The PCL and PCL–HA composite membranes showed a significant decrease in the intensity of the diffraction peaks in the first month, but there was no difference for the PCL–CoHA composite membranes. After immersion for one month, the intensity of the diffraction peaks of all samples decreased. The intensity of the diffraction peak [110] representing PCL is compared (Fig. 7F). Pure PCL has the highest crystallinity followed by PCL–CoHA and PCL–HA composite membranes, which is consistent with the DSC calculations (Table 2). The results also show that the diffraction peak intensity of PCL decreases with the increase of immersion time. This means that the crystal structure of PCL is destroyed.

3.6. *In vitro release of cobalt ions and anti-inflammatory evaluation*

The cobalt ion standard solution was added to the PBS and measured by UV–vis when a significant absorption band was

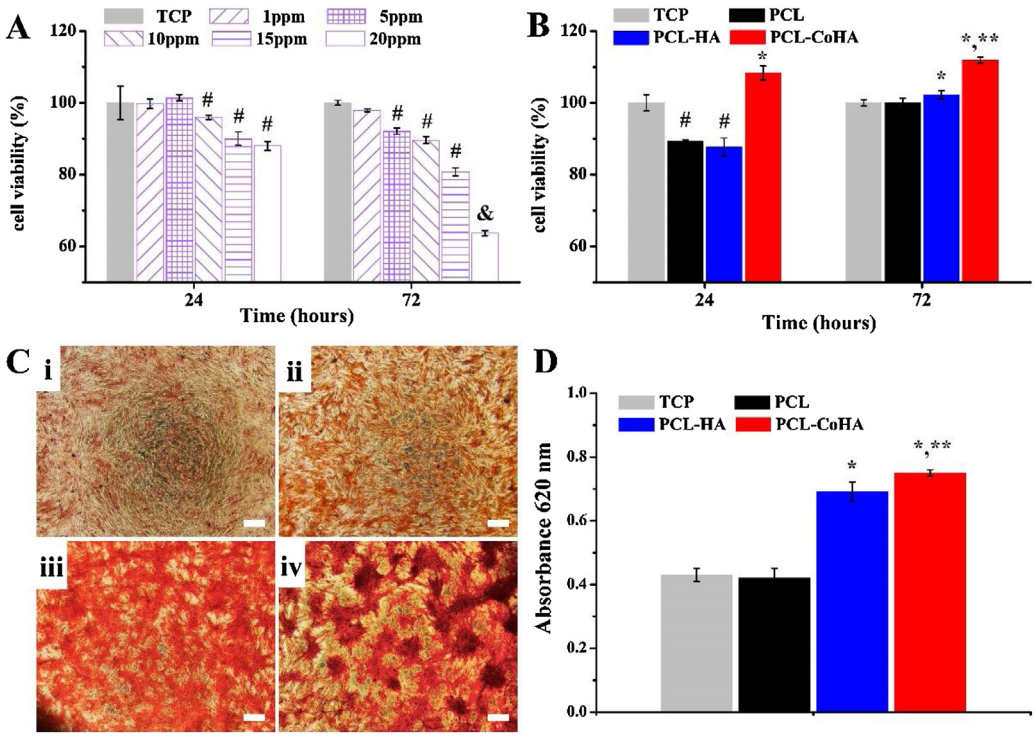

Fig. 4 – Comparison of MG63 cells proliferation on the (A) cobalt standard solution; (B) control sample (TCP), pure PCL, PCL–HA and PCL–CoHA composites membrane as determined by an MTT assay ($p < 0.05$, mean ± SD, $n = 3$). (C) Images of the ARS results for: (i) control (TCP), (ii) PCL, (iii) PCL–HA and (iv) PCL–CoHA composites membranes. Scale bars, 100 μm. The red districts present calcium mineralized on the composite membrane surfaces. (D) Quantitative analysis of matrix deposition mineralization was performed at 7 days. ($p < 0.05$, mean ± SD, $n = 4$) *: significantly higher than the control group (TCP) **: significantly higher than other groups. #: significantly lower than the control group &: significantly lower than other groups. (For interpretation of the references to colour in this figure legend, the reader is referred to the web version of this article).

observed at the position of 302 nm (Fig. 8A). Subsequently, the PBS solution after degradation of PCL, PCL–HA and PCL–CoHA composite membranes was determined. The results show that the release of cobalt ions is proportional to the time (Fig. 8B), confirming the release of cobalt ions. The cobalt ion standard solution was used to evaluate the free radical capture ability of cobalt ions. The free radical scavenging rate increases as the concentration of cobalt ions increases (Fig. 8C). With the increase of time, the scavenging rate of free radical in all samples continued to increase (Fig. 8D). The release of cobalt ions

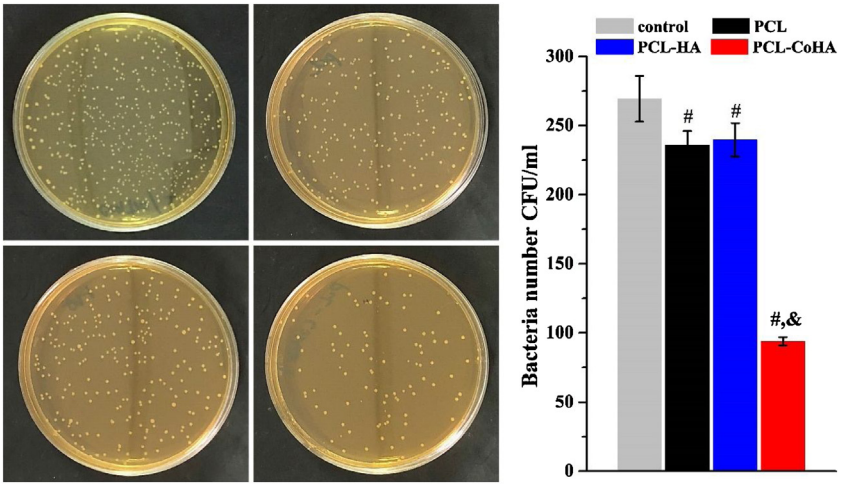

Fig. 5 – Images of the antibacterial results for relatively bacterial colonies on agar plates: (A) control (BHI), (B) PCL, (C) PCL–HA and (D) PCL–CoHA composites membranes. (E) Antibacterials activity of the analyzed composites membrane on *E. coli*. *: significantly lower than the control group. #: significantly lower than other groups. ($p < 0.05$, mean ± SD, $n = 4$).

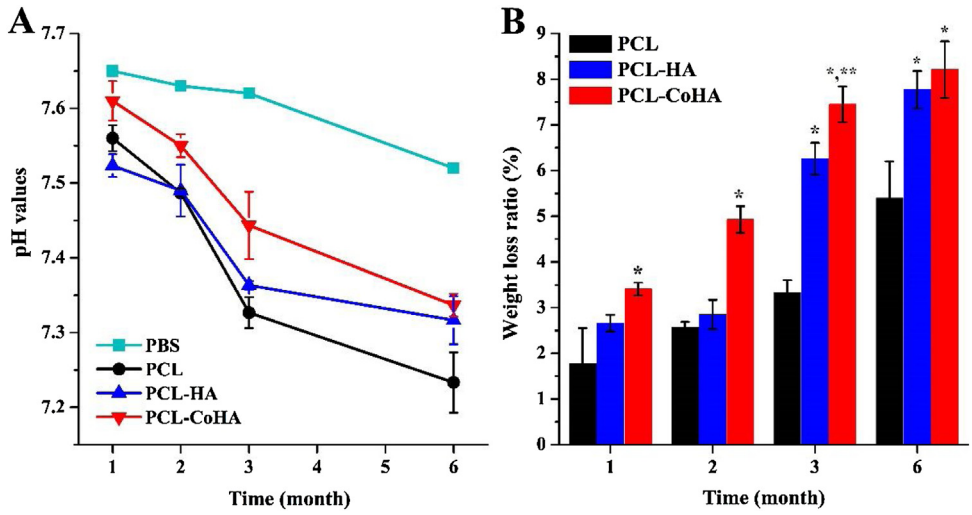

Fig. 6 – Biodegradation analysis of PCL, PCL–HA and PCL–CoHA composites membranes ; (A) change of pH value in PBS extraction solution, (B) weight loss of composite membrane. *: significantly higher than the PCL group. ($p < 0.05$, mean ± SD, n = 4). **: significantly higher than other groups.

caused PCL–CoHA composite membranes to be significantly higher than the other two groups at different times ($p < 0.05$). After 6 months, the free radical scavenging rate of PCL–CoHA was higher than PCL by about 18%.

4. Discussion

The purpose of the present study was to fabricate PCL composite membranes with cobalt ion as versatility regeneration membranes and to assess their effects on biocompatibility, antibacterial activity, biodegradability and anti-inflammatory evaluation. We surmised that composite membranes contained with cobalt-substituted hydroxyapatite would increase biological activity and reduce bacterial grow. For this aim, CoHA were loaded in PCL composite membranes and use the commodities HA as a control.

The powders of HA or CoHA added to the PCL membranes are exposed on the surface. These HAs are similar to the composition of human bones, release calcium and phosphorus ions after degradation, which can improve the biological activity of the material and promote the regeneration of bone tissue. PCL–HA and PCL–CoHA composite membrane showed a broad single peak at 1026 cm^{-1} using ATR-FTIR spectrum under the influence of PCL, indicating uniform mixing of powders with PCL. Observation of the crystal structure, the addition of powders disrupted the alignment of the PCL resulting in a decrease in crystallization. Moreover, since the powder of CoHA is not calcined, the crystallinity of CoHA is low. There is no obvious diffraction peak of CoHA in the XRD pattern of PCL–CoHA. However, low-crystalline CoHA is more susceptible to degradation, and release of ions is involved in tissue repair. The result of DSC displayed that the addition of HA and CoHA led to more sprocket entanglements, which restricted the chain mobility and crystallization of PCL. The lower crystallinity of PCL showed better mixedness of PCL and HA (or CoHA). This result was consistent with XRD patterns. Pure PCL had a higher crystallization but means that it is not easily degraded. The literature points out that pure PCL mass loss of about 24–36 months [39], so degradation of PCL can be accelerated by reducing crystallinity.

However, the use of cobalt ion concentration has safety concerns for the human body. The MTT test showed that the concentration of cobalt ions in the range of 15 ppm do not have a negative effect on the cells. Calculate the original added CoHA content, the cobalt ion concentration of the PCL–CoHA composite membrane was 0.4 ppm/cm^3 (much lower than 15 ppm), which is within a security concentration range. Adhesion and diffusion happen in the initial phase of biomaterial interaction and would affect the cell capability to proliferate on the material [31]. The viability of the cells proliferated on the membranes represented the biocompatibility of the composite membranes. The MG63 cells cultured on the membrane surface showed that the PCL–CoHA composite membrane significantly increased the number of cells by the release of cobalt ions, regardless of whether the cells were initial attachment or late hyperplasia. The calcium deposition performance of the observed cells for 7 day culture also had the same results. Previous studies have shown that cobalt ions can effectively activate the hypoxia-inducible factor 1-alpha (HIF-1α) protein expression, and induce the secretion of vascular endothelial growth factor (VEGF) to promote the growth of bone cells [40–42]. Nenad Ignjatovic et al. reported that hydrothermal synthesis of CoHA was implanted in the mandible of a rat model of osteoporosis, indicating that the mineral deposition rate of cobalt ion-filled sites is higher than that of pure Hap and accelerates the rate of bone formation [21,43]. The release of cobalt ions contributes to the growth and differentiation of bone cells on the PCL–CoHA composite membrane.

In addition to good biocompatibility, decreased postoperative infection is also a challenge for implantable biomedical materials. There is inevitably a presence of bacteria around the wound, causing infection of the wound. A common antibacterial method at present is the use of drugs [31] or metal ions

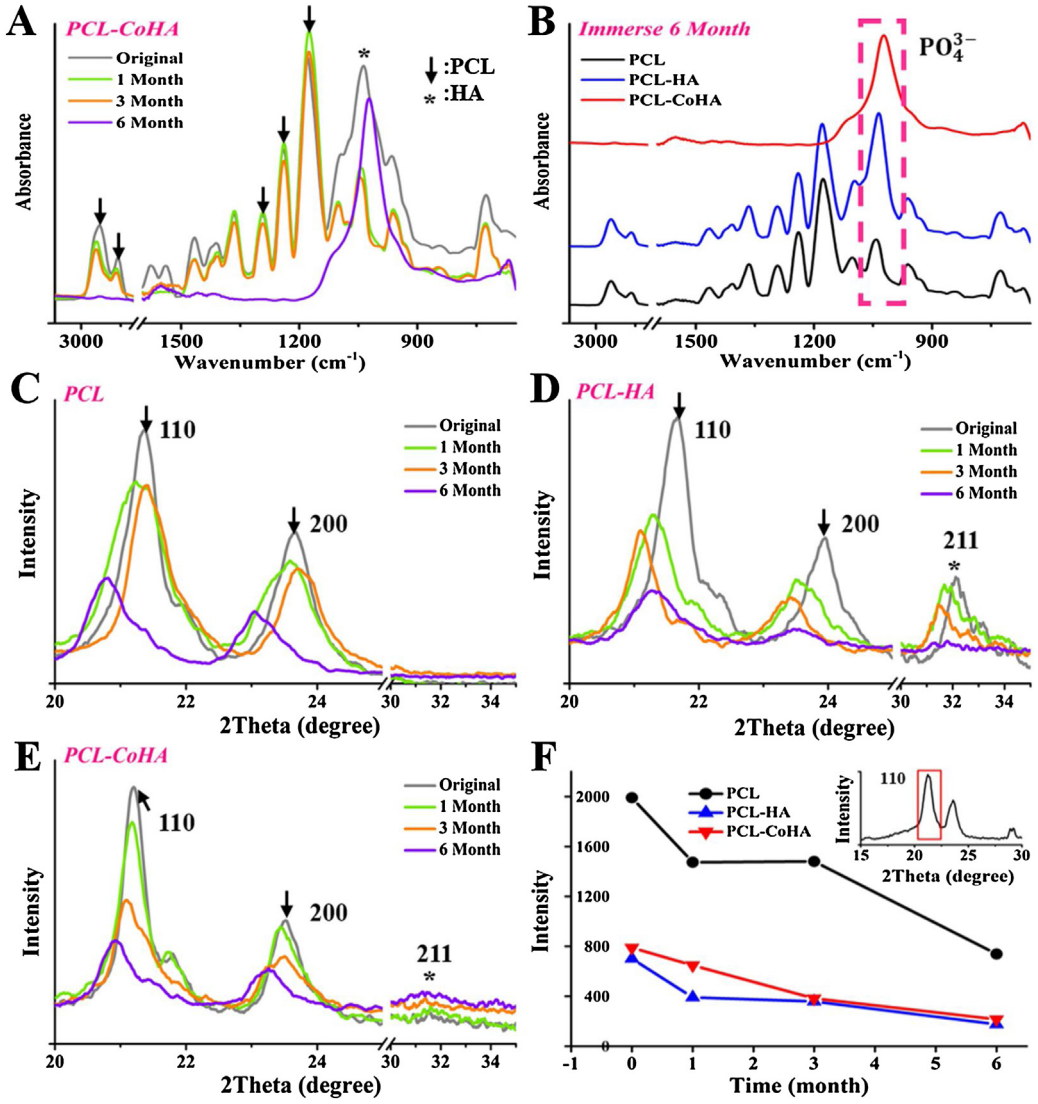

Fig. 7 – Calcium–phosphorus ratio and crystal structure of PCL, PCL-HA and PCL-CoHA composite membranes after degraded at different times; (A–B) FTIR spectra, (C–E) XRD patterns and (F) strength comparison of the PCL [110] peak.

[44]. Previous studies of cobalt oxide nan powders were found to be extremely efficient in inhibit *E. coli* by producing ROS [22]. The antibacterial results showed that PCL and PCL–HA did not have significant bactericidal effects, while PCL–CoHA significantly inhibited bacterial growth. This confirms that the antibacterial effect comes from the addition of cobalt ions. Furthermore, the PCL–CoHA composite membrane was confirmed to be non-toxic by the MTT test. Therefore, there is no produce a negative impact on the body.

Moreover, an appropriate function of many implantable regeneration membranes would be simultaneous of polymer degradation with the substitute by autologous tissue produced from cells [39]. To evaluate the degradation situation of the PCL–CoHA composite membranes and the release behavior of cobalt ions by long-term immersion in PBS. PCL–CoHA composite membrane induces recrystallization of ions in PBS by releasing cobalt ions and calcium ions after soaking for 6 months. A new calcium phosphate crystal was formed on the surface. It showed that PCL can enhance biological activity by adding CoHA. The environmental impact of membrane degradation was assessed by pH value in PBS solution. The release of oleic acid in PCL would cause the solution to become acidic. The HA and CoHA contain alkaline phosphorus ions, and the release of phosphorus ions alleviates the decrease in the pH value of PBS in PCL–HA and PCL–CoHA composite membranes. The literature indicated that *in vivo*, acid degradation may lead to the occurrence of ammatory reactions [39]. Added HA and CoHA can help to prevent the formation of unfavorable surroundings for the cells due to a decreased pH.

Previous studies have shown that the weight loss of PCL is not much in a neutral environment (pH 7) [35]. Therefore, the introduction of HA and CoHA in this experiment increased the loss of PCL. The change in the structure of the membrane was evaluated by XRD. The intensity of the diffraction peak of PCL decreased after soaking, indicating that the membrane was degraded. Literature pointed out the structure of the GTR membrane must be maintained for at least 4–6 weeks to allow

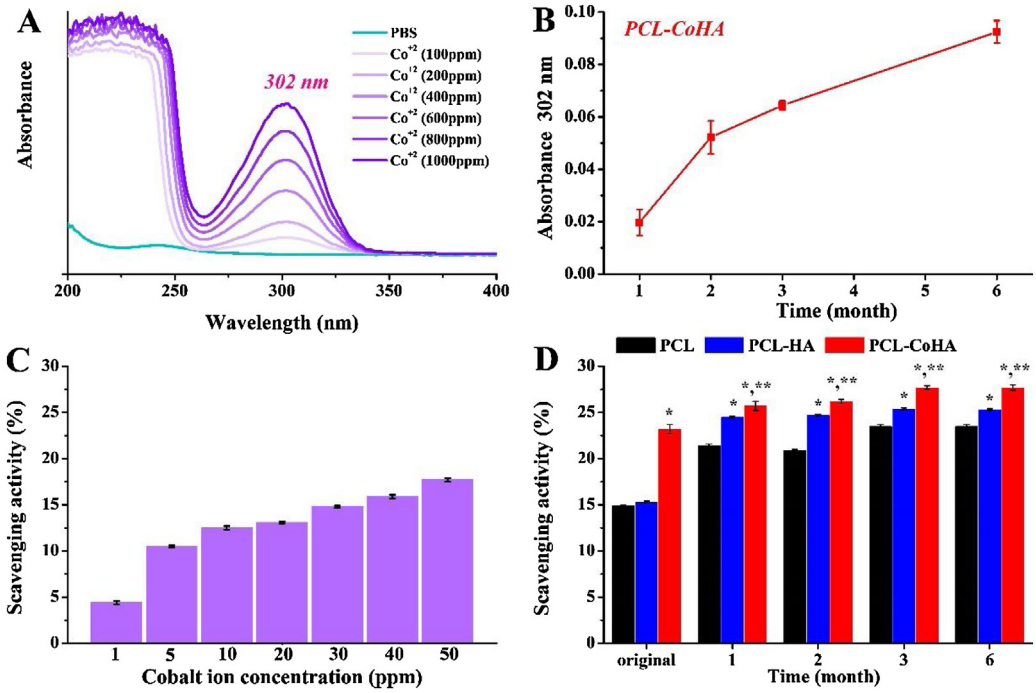

Fig. 8 – The cobalt ion absorption intensity by UV–vis; (A) cobalt standard solution, (B) PBS solutions of PCL–CoHA composite membranes after degraded. Free scavenging ratios of (C) cobalt standard solution; (D) original composite membranes and PBS solutions of different composite membranes degradation. *: significantly higher than the PCL group. **: significantly higher than other groups. ($p < 0.05$, mean ± SD, n = 4).

successful regeneration of periodontal tissue [45]. It shows that the maintenance of the structure of PCL–CoHA composite membranes is in the range of 4–6 weeks, which accord the GTR requirement. As time increases, the two peaks of PCL move slightly to a low angle to indicate that they belong to PCL with high crystallinity [30]. This result showed that the low crystalline PCL on the membrane surface is decomposed after degradation. The changes of diffraction peak intensity of PCL, PCL–CoHA and PCL–CoHA composite membranes were observed with time. Pure PCL is still the highest among PCL–HA and PCL–CoHA in crystallization strength after 6 months of degradation. This means that the degradation of pure PCL is limited. In addition, to confirm the release of cobalt ions in PCL–CoHA composite membrane, we measured the degraded PBS using UV–vis. The results confirmed that cobalt ions were continuously released over time.

Recently, the anti-inflammatory effect of implantable biomedical materials has attracted more attention. Free radicals are produced during biological differentiation and defense; however, too many free radicals may cause excessive oxidation. Antioxidants can be used to maintain the normal growth of organisms by capturing harmful free radicals; thus, they play an important role in this balance. The cobalt ion standard solution confirmed that cobalt ions effectively capture free radicals. The initial clearance rate of PCL–CoHA composite membrane was 1.6 times higher than that of PCL. That is to say, the PCL–CoHA composite membrane can reduce the presence of free radicals at the beginning and indirectly reduce the occurrence of inflammation. Subsequent testing with PBS after degradation showed that PCL–CoHA was significantly higher than the other groups and increased clearance over time.

In summary, we developed a new biodegradable membrane containing CoHA and explored the physicochemical properties of the membrane and its long-term degradation change. The above results indicate that the PCL–CoHA composite membrane contributes to cell attachment, differentiation and inhibition of antibacterial growth by the release of cobalt ions. The long-term degradation of the PCL composite membranes shows that the PCL–CoHA composite membrane surface can induce calcium phosphate deposition, combined with the acid neutralization, accelerated degradation and continuous scavenging free radicals to reduce the chance of inflammation. Meanwhile, these results support our hypothesis that the addition of CoHA is significantly effective against the antibacterial and anti-inflammatory properties of the membranes.

5. Conclusions

In this study, we developed a PCL–CoHA composite membranes. Reduce the crystallinity and increase the degradability of the PCL membrane by introducing a tiny amount of CoHA. We also confirmed that cobalt ions in the PCL–CoHA composite membrane contribute to the differentiation of bone cells and inhibit the growth of *E. coli*. At the same time, the PCL–CoHA composite membranes reduce the incidence of inflammatory reactions by continuously releasing cobalt ions and effectively reducing the production of free radicals. Based on the fact that the PCL–CoHA composite membrane possessing exceptional biocompatibility, antibacterial effect and anti-inflammatory

properties. Therefore, the PCL–CoHA composite membrane described in this study can be considered as an ideal choice for GBR regeneration membranes. It is expected that there will be very promising to be used in the clinical in the future.

REFERENCES

[1] Gentile P, Chiono V, Tonda-Turo C, Ferreira AM, Ciardelli G. Polymeric membranes for guided bone regeneration. Biotechnol J 2011;6:1187–97.
[2] Sarasam A, Madihally SV. Characterization of chitosan–polycaprolactone blends for tissue engineering applications. Biomaterials 2005;26:5500–8.
[3] Okamoto M, John B. Synthetic biopolymer nanocomposites for tissue engineering scaffolds. Prog Polym Sci 2013;38:1487–503.
[4] Ma PX. Biomimetic materials for tissue engineering. Adv Drug Deliv Rev 2008;60:184–98.
[5] Abou Neel EA, Bozec L, Knowles JC, Syed O, Mudera V, Day R, et al. Collagen—emerging collagen based therapies hit the patient. Adv Drug Deliv Rev 2013;65:429–56.
[6] Zhang Q, Jiang Y, Zhang Y, Ye Z, Tan W, Lang M. Effect of porosity on long-term degradation of poly (ε-caprolactone) scaffolds and their cellular response. Polym Degrad Stab 2013;98:209–18.
[7] Bhavsar MD, Amiji MM. Development of novel biodegradable polymeric nanoparticles-in-microsphere formulation for local plasmid DNA delivery in the gastrointestinal tract. AAPS PharmSciTech 2008;9:288–94.
[8] Moers-Carpi MM, Sherwood S. Polycaprolactone for the correction of nasolabial folds: a 24-month, prospective, randomized, controlled clinical trial. Dermatol Surg 2013;39:457–63.
[9] Roohani-Esfahani S-I, Nouri-Khorasani S, Lu Z, Appleyard R, Zreiqat H. The influence hydroxyapatite nanoparticle shape and size on the properties of biphasic calcium phosphate scaffolds coated with hydroxyapatite—PCL composites. Biomaterials 2010;31:5498–509.
[10] Liu C, Xia Z, Czernuszka J. Design and development of three-dimensional scaffolds for tissue engineering. Chem Eng Res Des 2007;85:1051–64.
[11] Rezwan K, Chen Q, Blaker J, Boccaccini AR. Biodegradable and bioactive porous polymer/inorganic composite scaffolds for bone tissue engineering. Biomaterials 2006;27:3413–31.
[12] Marcacci M, Kon E, Zaffagnini S, Giardino R, Rocca M, Corsi A, et al. Reconstruction of extensive long-bone defects in sheep using porous hydroxyapatite sponges. Calcif Tissue Int 1999;64:83–90.
[13] Campoccia D, Montanaro L, Arciola CR. A review of the biomaterials technologies for infection-resistant surfaces. Biomaterials 2013;34:8533–54.
[14] Wang Y, Yang X, Gu Z, Qin H, Li L, Liu J, et al. In vitro study on the degradation of lithium-doped hydroxyapatite for bone tissue engineering scaffold. Mater Sci Eng C Mater Biol Appl 2016;66:185–92.
[15] Sumathi S, Gopal B. In vitro degradation of multisubstituted hydroxyapatite and fluorapatite in the physiological condition. J Cryst Growth 2015;422:36–43.
[16] Kramer ER, Morey AM, Staruch M, Suib SL, Jain M, Budnick JI, et al. Synthesis and characterization of iron-substituted hydroxyapatite via a simple ion-exchange procedure. J Mater Sci 2013;48:665–73.
[17] Klasen H. Historical review of the use of silver in the treatment of burns. I. Early uses. Burns 2000;26:117–30.
[18] Chandran S, Shenoy SJ, Babu SS, PN R, KV H, John A. Strontium hydroxyapatite scaffolds engineered with stem cells aid osteointegration and osteogenesis in osteoporotic sheep model. Colloids Surf B Biointerfaces 2018;163:346–54.
[19] Carson BL, Ellis IIIHV, McCann JL. Toxicology and biological monitoring of metals in humans; 1986.
[20] Wu C, Zhou Y, Fan W, Han P, Chang J, Yuen J, et al. Hypoxia-mimicking mesoporous bioactive glass scaffolds with controllable cobalt ion release for bone tissue engineering. Biomaterials 2012;33:2076–85.
[21] Ignjatović N, Ajduković Z, Savić V, Najman S, Mihailović D, Vasiljević P, et al. Nanoparticles of cobalt-substituted hydroxyapatite in regeneration of mandibular osteoporotic bones. J Mater Sci Mater Med 2013;24:343–54.
[22] Kavitha T, Haider S, Kamal T, Ul-Islam M. Thermal decomposition of metal complex precursor as route to the synthesis of Co_3O_4 nanoparticles: antibacterial activity and mechanism. J Alloys Compd 2017;704:296–302.
[23] Lin W-C, Chuang C-C, Wang P-T, Tang C-M. A comparative study on the direct and pulsed current electrodeposition of cobalt-Substituted hydroxyapatite for magnetic resonance imaging application. Materials 2018;12:116.
[24] Zhou J, Zhao L. Hypoxia-mimicking Co doped TiO_2 microporous coating on titanium with enhanced angiogenic and osteogenic activities. Acta Biomater 2016;43:358–68.
[25] Brand-Williams W, Cuvelier M-E, Berset C. Use of a free radical method to evaluate antioxidant activity. LWT Food Sci Technol 1995;28:25–30.
[26] Tang C-M, Tian Y-H, Hsu S-H. Poly(vinyl alcohol) nanocomposites reinforced with bamboo charcoal nanoparticles: mineralization behavior and characterization. Materials 2015;8:4895–911.
[27] Stanić V, Radosavljević-Mihajlović AS, Živković-Radovanović V, Nastasijević B, Marinović-Cincović M, Marković JP, et al. Synthesis, structural characterisation and antibacterial activity of Ag+-doped fluorapatite nanomaterials prepared by neutralization method. Appl Surf Sci 2015;337:72–80.
[28] Kolmas J, Piotrowska U, Kuras M, Kurek E. Effect of carbonate substitution on physicochemical and biological properties of silver containing hydroxyapatites. Mater Sci Eng C Mater Biol Appl 2017;74:124–30.
[29] Ishikawa K. Bone substitute fabrication based on dissolution-precipitation reactions. Materials 2010;3:1138–55.
[30] Xue J, He M, Liu H, Niu Y, Crawford A, Coates PD, et al. Drug loaded homogeneous electrospun PCL/gelatin hybrid nanofiber structures for anti-infective tissue regeneration membranes. Biomaterials 2014;35:9395–405.
[31] Xue J, Shi R, Niu Y, Gong M, Coates P, Crawford A, et al. Fabrication of drug-loaded anti-infective guided tissue regeneration membrane with adjustable biodegradation property. Colloids Surf B Biointerfaces 2015;135:846–54.
[32] Heydari Z, Mohebbi-Kalhori D, Afarani MS. Engineered electrospun polycaprolactone (PCL)/octacalcium phosphate (OCP) scaffold for bone tissue engineering. Mater Sci Eng C Mater Biol Appl 2017;81:127–32.
[33] Meng ZX, Zheng W, Li L, Zheng YF. Fabrication and characterization of three-dimensional nanofiber membrance of PCL–MWCNTs by electrospinning. Mater Sci Eng C 2010;30:1014–21.
[34] Sarath Chandra V, Elayaraja K, Thanigai Arul K, Ferraris S, Spriano S, Ferraris M, et al. Synthesis of magnetic hydroxyapatite by hydrothermal—microwave technique: dielectric, protein adsorption, blood compatibility and drug release studies. Ceram Int 2015;41:13153–63.
[35] Scaffaro R, Lopresti F, Botta L. Preparation, characterization and hydrolytic degradation of PLA/PCL co-mingled nanofibrous mats prepared via dual-jet electrospinning. Eur Polym J 2017;96:266–77.

[36] Ortali C, Julien I, Vandenhende M, Drouet C, Champion E. Consolidation of bone-like apatite bioceramics by spark plasma sintering of amorphous carbonated calcium phosphate at very low temperature. J Eur Ceram Soc 2018;38:2098–109.
[37] He D-H, Wang P, Liu P, Liu X-K, Ma F-C, Zhao J. HA coating fabricated by electrochemical deposition on modified Ti6Al4V alloy. Surf Coat Technol 2016;301:6–12.
[38] Leyssens L, Vinck B, Van Der Straeten C, Wuyts F, Maes L. Cobalt toxicity in humans—a review of the potential sources and systemic health effects. Toxicology 2017;387:43–56.
[39] Hutmacher DW. Scaffolds in tissue engineering bone and cartilage. Biomaterials 2000;21:2529–43.
[40] Dai Y, Li W, Zhong M, Chen J, Liu Y, Cheng Q, et al. Preconditioning and post-treatment with cobalt chloride in rat model of perinatal hypoxic–ischemic encephalopathy. Brain Dev 2014;36:228–40.
[41] Loboda A, Jazwa A, Wegiel B, Jozkowicz A, Dulak J. Heme oxygenase-1-dependent and-independent regulation of angiogenic genes expression: effect of cobalt protoporphyrin and cobalt chloride on VEGF and IL-8 synthesis in human microvascular endothelial cells. Cell Mol Biol (Noisy-le-grand) 2005;51:347.
[42] Tanaka T, Kojima I, Ohse T, Ingelfinger JR, Adler S, Fujita T, et al. Cobalt promotes angiogenesis via hypoxia-inducible factor and protects tubulointerstitium in the remnant kidney model. Lab Investig 2005;85:1292–307.
[43] Ignjatovic N, Ajdukovic Z, Rajkovic J, Najman S, Mihailovic D, Uskokovic D. Enhanced osteogenesis of nanosized cobalt-substituted hydroxyapatite. J Bionic Eng 2015;12:604–12.
[44] Hou X, Ma H, Liu F, Deng J, Ai Y, Zhao X, et al. Synthesis of Ag ion-implanted TiO_2 thin films for antibacterial application and photocatalytic performance. J Hazard Mater 2015;299:59–66.
[45] Sculean A, Nikolidakis D, Schwarz F. Regeneration of periodontal tissues: combinations of barrier membranes and grafting materials—biological foundation and preclinical evidence: a systematic review. J Clin Periodontol 2008;35:106–16.